Pressure loss and performance assessment of horizontal spiral coil inserted pipes during forced convective evaporation of R-600a

Article (Accepted Version)

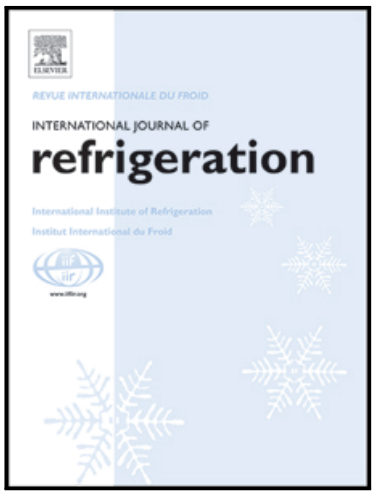

Pressure loss and performance assessment of horizontal spiral coil inserted pipes during forced convective evaporation of R-600a

Farzam Alimardani , Hadi Ahmadi Moghaddam ,
Alireza Sarmadian , Maziar Shafaee

PII: S0140-7007(19)30353-6
DOI: https://doi.org/10.1016/j.ijrefrig.2019.08.016
Reference: JIJR 4496

To appear in: *International Journal of Refrigeration*

Received date: 19 May 2019
Revised date: 9 August 2019
Accepted date: 12 August 2019

Please cite this article as: Farzam Alimardani , Hadi Ahmadi Moghaddam , Alireza Sarmadian , Maziar Shafaee , Pressure loss and performance assessment of horizontal spiral coil inserted pipes during forced convective evaporation of R-600a, *International Journal of Refrigeration* (2019), doi: https://doi.org/10.1016/j.ijrefrig.2019.08.016

Highlights

- Spiral coils usage resulted in the pressure loss increase.
- Using inserts is beneficial at higher mass fluxes.
- The maximum performance factor of 1.4 was obtained by using inserts.
- A correlation for evaporative pressure drop of R-600a in rough pipes was developed.

Pressure loss and performance assessment of horizontal spiral coil inserted pipes during forced convective evaporation of R-600a

Farzam Alimardani [a,b], Hadi Ahmadi Moghaddam [a,b], Alireza Sarmadian [c], Maziar Shafaee*[a]

[a]Faculty of New Sciences and Technologies, University of Tehran, Tehran, Iran
[b]Center of Excellence in Design and Optimization of Energy Systems, School of Mechanical Engineering, College of Engineering, University of Tehran, Tehran, Iran
Email: f.alimardani@alumni.ut.ac.ir, ahmadi.hadi@ut.ac.ir
[c]Department of Engineering and Design, University of Sussex, Brighton BN1 9QT, UK
Email: a.sarmadian@sussex.ac.uk
*Corresponding Author, Email: mshafaee@ut.ac.ir, Tel.: +98-919-0110200; fax: +98-21-88497324

Abstract

The impacts of spiral coil inserts on the pressure loss of environment-friendly refrigerant R-600a are experimentally evaluated during forced convective evaporation within horizontal copper pipes. Then, by considering the current pressure drop and previous heat transfer results and calculating the performance factor, the overall effectiveness of the inserts is determined. Experiments are carried out for smooth and rough tubes. Five spiral coils with various coil pitches and wire diameters are utilized. Also, vapor qualities between 0.08-0.7 and mass fluxes between 109.2-505 $kgm^{-2}s^{-1}$ are considered for tests. Generally, it is observed that inserts augment the pressure loss in the range of 90-958% over the smooth pipe. However, as the wire diameter decreases and the coil pitch increases, less pressure losses are imposed to the system. Depending on the operational conditions and inserts type, the performance factor was obtained between 0.13-1.40. The coiled wire "CW5" with the wire diameter of 1 *mm* and coil pitch of 30 *mm* performed superior compared to the other inserts by maximum performance factor of 1.4. Finally, by using the current data a new correlation is proposed in order to predict the evaporative pressure loss of R-600a within spiral coil inserted pipes.

Keywords: *Correlation; Evaporation; Pressure loss; R-600a; Spiral coil*

Nomenclature

d	tube diameter (mm)
e	wire diameter (m)
G	mass velocity ($kgm^{-2}s^{-1}$)
I	electric current (A)
p	pressure (kPa)
P	coil pitch (m)
V	electric voltage (V)
x	vapor quality

Greek symbols

θ	helix angle of coiled wire ($degree$)
η	Efficiency of insulation
ε	Steiner void fraction
ρ	density
σ	surface tension

Subscripts

c	coiled wire insert
e	equivalent
ev	evaporator
$fric$	frictional
g	vapor phase
i	inner
in	inlet
l	liquid phase
mom	momentum
o	outlet
ph	preheater
ref	refrigerant
s	smooth
tot	total

1. Introduction

During recent years, growing concerns associated with environmental issues such as ozone depletion have led to extensive use of environment-friendly refrigerants. First, CFC and HCFC refrigerants were replaced by HFC refrigerants. However, utilizing HFCs has reduced, although the ozone depleting potential (ODP) of these fluids is zero. For instance, despite the preferable thermodynamic properties of R-134a as a widely-used HFC refrigerant, its usage in different domestic and industrial applications has to be declined because the global warming potential (GWP) of this refrigerant is high. Therefore, the tendency to use natural refrigerants such as R-600a (Isobutane) has increased recently.

Besides, investigating the thermal systems performance such as heat-exchangers for less energy usage is a crucial factor. Employing modified surfaces like dimpled pipes [1], corrugated pipes [2] and micro-fin pipes [3] or installing inserts like coiled wires [4] and twisted tapes [5] inside heat-exchangers are examples of techniques for such a purpose. Using these methods as passive techniques of heat transfer enhancement does not require an external power as it is required in active methods [6, 7]. The inserts such as coiled wires are employed in heat-exchangers as turbulators to increase the heat transfer rate. There is a tendency among researchers to use spiral coils because these devices are low in cost and effective [8]. However, the downside of these methods is inducing a considerable amount of pressure drop which must be taken into account for an appropriate designing. In this regard, different prediction methods are developed to help the researchers in designing efficient heat-exchangers.

Refrigerant R-600a has several merits which make it an appropriate candidate for use in refrigeration systems. The liquid density of R-600a is less than most of the fluorocarbon refrigerants. Therefore, the charge amounts would be reduced considerably using R-600a that would contribute to further relieving the emissions of the refrigerant directly [9]. The thermal conductivity of R-600a is larger than that of some other refrigerants as R-134a and R-22 which would result in better heat transfer performance. Also, having smaller liquid viscosity helps higher liquidity in heat exchangers [10]. Another advantage of R-600a over R-134a is that R-600a has a larger latent heat. For a fluid which has a higher latent heat, less mass flow rates would be required in order to produce a specific capacity [11, 12]. Although R-600a is flammable and this can become a concern, but it should be noticed that a huge volume of this fluid is used safely every day in entire the world in different applications such as heating or cooking [13].

Considering the above-mentioned advantages of R-600a, many experiments have been already carried out to reveal the performance of two-phase flow heat exchangers working with this refrigerant. Copetti et al. [14] conducted an empirical investigation on horizontally installed pipes using R-600a, when different heat fluxes, mass fluxes and vapor qualities were applied to the system. It was found that the transferred heat and pressure loss are dependent of the system operational conditions. Furthermore, compared with R-134a, the obtained coefficient of heat transfer and pressure losses are higher for R-600a. Within another experimental research on

tubes with porous inserts and by using R-600a, Wen et al. [15] reported that by increment of the mass flux and applied heat, and decrement of the vapor quality, the heat transfer augments. Also, the inserts give rise to the pressure loss. Finally, based on the presented data, experimental correlations were suggested so as to predict the pressure losses and coefficients of heat transfer for Isobutane. Shafaee et al. [16] experimentally appraised the flow boiling heat transfer performance of a heat-exchanger working with R-600a. In this research, spiral coils with varied geometrical features were utilized inside horizontally located pipes. The results showed that inserting the wire coils and augmenting the vapor quality and mass velocity contribute to the increment of the heat transfer coefficients. In another empirical study performed by Shafaee et al. [17] on boiling of R-600a in plain and rough pipes, it was demonstrated that heat transfer rate and pressure drops in dimpled pipes are larger than those obtained in smooth pipes. To illustrate the impacts of operational conditions and pipe surface roughness on the magnitude of heat transfer coefficient and pressure loss obtained during condensation of R-600a, Sarmadian et al. [18] evaluated a two-phase flow heat-exchanger. According to the observations, increasing the vapor quality and mass flux gives rise to the rate of transferred heat and pressure loss. Also, the rough surfaces lead to augmentation in both pressure losses and heat transfer coefficients compared to the smooth surfaces. Oliveira et al. [19] assessed the pressure loss of refrigerants R-290 and R-600a during evaporation inside a horizontal pipe; when the mass velocity was changing between 240-480 $kgm^{-2}s^{-1}$, and the applied heat flux to the test section was changing between 5-60 kWm^{-2}. Experiments demonstrated a larger pressure drop for R-600a for all tests operating conditions. It was also observed that increasing the mass velocity and vapor quality gives rise to the pressure drops for both working fluids. To compare the performance of refrigerants R-600a and R1234ze(E), Yang et al. [20] conducted an empirical study on horizontally installed pipes. For this purpose, tests were performed under various saturation pressures, heat fluxes, and mass velocities. As a result, it was observed that compared to R1234ze(E), R-600a usage results in higher heat transfer rates and pressure losses.

Despite the numerous efforts made previously for investigating the performance of heat-exchangers with R-600a, there is no reported research on evaporative pressure drop of R-600a in spiral coil inserted tubes. In this research firstly, the pressure drop growth of R-600a during forced convection evaporation in horizontal smooth and spring inserted pipes (rough pipes) is studied. Then, the performance of rough pipes is evaluated by considering the previous results of Shafaee et al. [16], to illuminate the overall effectiveness of these inserts. Finally, an experimental correlation is suggested based on the current empirical data in order to predict the pressure drop of R-600a during evaporation in horizontal tubes with spiral coils.

2. Test setup design

The overall schematic view of the test setup is illustrated in Fig. 1. Preheaters, test evaporator, sight glass, condenser, flow meter, gear pump, pressure and temperature sensors, and differential pressure drop transducer are the main components constituting the cycle. R-600a is used in the cycle as the refrigerant and water is used as the coolant for eliminating the latent heat from R-600a. The purity of R-600a was about 99.5%. In order to circulate the refrigerant in the cycle, a variable frequency gear pump was installed after the condenser. Also, a flow meter was placed

before the preheaters for measuring the refrigerant mass flow rate. Two electrical resistance preheaters were used prior to test evaporator to reach the required vapor quality at the test section inlet. The studied test evaporator was a horizontally installed pipe constructed from copper with the length, internal diameter, and wall thickness of 1000, 8.1, and 0.71 *mm*, respectively. To minimize the heat losses to the environment, the test pipe was insulated using glass wool pad. A sight glass was also placed just after the test tube for observing the flow patterns.

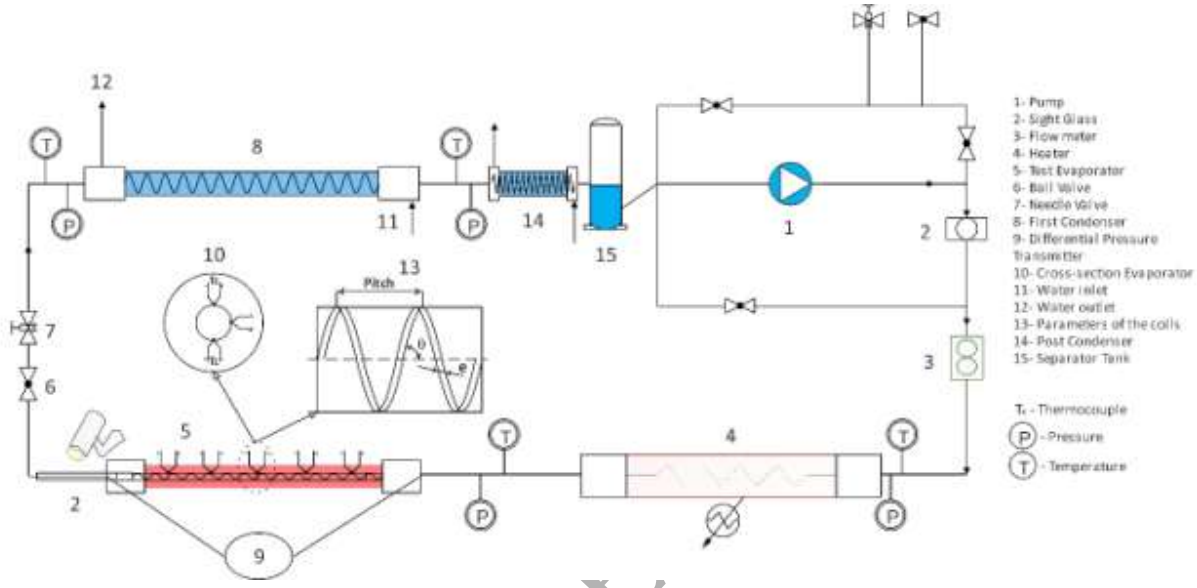

Fig. 1. Schematic view of the test setup

To measure the wall temperature of the test tube, K-type thermocouples were attached to the tube by welding at five axial locations with a distance of 200 *mm* from each other. In this regard, at each axial location, four thermocouples were attached to the bottom, top and two sides of the pipe. To determine the pressure drop during the test section, a differential pressure drop transducer was installed in the cycle. Further information regarding the test setup can be found in [16].

Experiments were performed on horizontal smooth and spiral coil inserted pipes. In this regard, five circular cross-section springs with various geometrical features, i.e. varied coil pitches and wire diameters, were installed inside the test pipes. The features of the test pipes and spiral coils examined in this research are presented in Table 1.

Table 1. Geometrical parameters of the spiral coil inserted pipes

Tube set	e (*mm*)	P (*mm*)	θ (degree)	d_i (*mm*)
Plain	-	-	-	8.1
CW1	0.5	10	67.27	8.1
CW2	1	10	65.85	8.1
CW3	1.5	10	64.25	8.1
CW4	1	20	48.12	8.1
CW5	1	30	36.63	8.1

The experimental results of plain and rough tubes are obtained for vapor qualities between 0.08-0.7 and mass fluxes between 109.2-505 $kgm^{-2}s^{-1}$. The operational conditions of the current test cycle are illustrated in Table 2.

Table 2. The ranges of governing operating conditions in this research

Refrigerant	R-600a
Heat flux (kWm^{-2})	18.6-26.1
Pressure (bar)	4-6
Vapor quality	0.08-0.70
Mass velocity ($kgm^{-2}s^{-1}$)	109.2-505

3. Data reduction

This experimental research is conducted to determine the pressure drop rise of refrigerant R-600a during its evaporation within smooth and spiral coil inserted pipes which are installed horizontally. During tests, the vapor quality changed between 0.08-0.7. Also, mass velocities of 109.2, 189, 269.5, 350.4, 431.3, and 505 $kgm^{-2}s^{-1}$ were considered for performing tests. The data were taken 15 minutes after the system initial start-up so that it can reach the steady state condition.

It is worth mentioning that the experiments have to be repeatable to collect the steady-state data. All experimental test loops have a limited range in which steady-state test conditions can be maintained. At low or high mass velocities, typically a threshold is reached where fluctuations in pressure and flow rate become significant. In particular, pressure fluctuations significantly influence T_{sat}, which makes the data unreliable. As it was mentioned by Thome et al. [21], it is particularly difficult to accurately measure the data at vapor qualities less than 0.05 and above 0.95. However, it is valid under ideal condition of a test section without springs (plain tube) or any inserts disruptive to flow field which has a potential to cause more fluctuations in the pressure drop and therefore make the measurements much trickier. In the present experimental measurements, trying to check the repeatability of the collected data under the same operating conditions, it was observed that the data above the vapor quality of 0.7 and less than 0.08 are not repeatable mostly for higher mass fluxes for the inserted tubes. Therefore, to maintain consistency and make the performance assessment possible, the ranges of vapor qualities and mass velocities were confined.

As it was discussed previously, the preheater was insulated to reduce the heat leakage to the environment. However, the thermal efficiency of the preheater was calculated as follows:

$$\eta = \frac{\dot{m}_{ref}(h_{ev,o} - h_{ph,i})}{Q_{el}} \quad (1)$$

In Eq. (1), $\dot{m}_{ref}$ is the refrigerant mass flow rate. $h_{ev,o}$ and $h_{ph,i}$ are the enthalpy of refrigerant at the test evaporator outlet and the preheater inlet, respectively. Also, Q_{el} represents the heat delivered by the electrical heaters.

The mean of vapor qualities at the test evaporator boundaries is considered as the vapor quality of the whole test section, as follows:

$$x = \frac{x_{ev,o} + x_{ev,i}}{2} \tag{2}$$

Where the vapor quality at the test section inlet and outlet are showed by $x_{ev,i}$ and $x_{ev,o}$, respectively.

To compute the vapor quality at the evaporator inlet and outlet, the following relations are used:

$$Q_{ph} = \eta(VI)_{ph} = Q_{sen} + Q_{lat} \tag{3}$$

$$Q_{sen} = C_P \dot{m}_{ref}(T_{sat,ph} - T_{ph,i}) \tag{4}$$

$$Q_{lat} = \dot{m}_{ref} h_{fg,ph} x_{ev,i} \tag{5}$$

By substituting Eq. (5) and Eq. (4) in Eq. (3), the vapor quality at the test evaporator inlet is determined as:

$$x_{ev,i} = \frac{Q_{ph} - C_P \dot{m}_{ref}(T_{sat,ph} - T_{ph,i})}{\dot{m}_{ref} h_{fg,ph}} \tag{6}$$

Also, the vapor quality at the test evaporator outlet is computed as follows:

$$x_{ev,o} = x_{ev,i} + {\eta(VI)_{ev}}\Big/{h_{fg,ev}} \tag{7}$$

Where Q_{ph}, Q_{sen}, Q_{lat}, C_P, $T_{sat,ph}$, $T_{ph,i}$, $h_{fg,ph}$, and $h_{fg,ev}$ represent the total transferred heat in preheater, sensible heat, latent heat, refrigerant specific heat associated with the mean temperature of the preheater, refrigerant saturation temperature associated with the mean pressure of the preheater, refrigerant temperature at preheater inlet, refrigerant vaporizing enthalpy associated with the mean pressure of the preheater, and refrigerant vaporizing enthalpy associated with the mean pressure of the test evaporator, respectively.

The total pressure drop of the test tube is as follows:

$$\Delta P_{tot} = \Delta P_{mom} + \Delta P_{stat} + \Delta P_{fric} \tag{8}$$

Where ΔP_{mom}, ΔP_{stat}, and ΔP_{fric} represent momentum, static, and frictional pressure drops, respectively.

The static pressure drop, ΔP_{stat}, is zero because the test tube is horizontal. Therefore:

$$\Delta P_{tot} = \Delta P_{mom} + \Delta P_{fric} \tag{9}$$

The suggested relation by Collier and Thome [22] is used for calculating the momentum pressure loss:

$$\Delta P_{mom} = G_{tot}^2 \left\{ \left[\frac{(1-x)^2}{\rho_l(1-\varepsilon)} + \frac{x^2}{\rho_g \varepsilon} \right]_{out} - \left[\frac{(1-x)^2}{\rho_l(1-\varepsilon)} + \frac{x^2}{\rho_g \varepsilon} \right]_{in} \right\} \tag{10}$$

In Eq. (10), x, ρ, and ε represent the vapor quality, density, and the void fraction, respectively. Also, G shows the mass velocity.

Furthermore, Eq. (11) introduced by Steiner [23] is utilized for calculating the void fraction. This correlation can be used for wide range of flow regimes:

$$\varepsilon = \frac{x}{\rho_g} \left\{ [1 + 0.12(1-x)] \left(\frac{x}{\rho_g} + \frac{1-x}{\rho_l} \right) + \frac{1.18(1-x)[g\sigma(\rho_l - \rho_g)]^{0.25}}{G_{tot}^2 \rho_l^{0.5}} \right\}^{-1} \tag{11}$$

By subtracting the momentum pressure drop from total pressure drop obtained from experiments, the frictional pressure losses can be determined.

Finally, the proposed method by Moffat [24] is used so as to calculate the uncertainties in determining pressure drops during tests. According to the calculations, the uncertainties were below 10% for all experiments.

Table 3. Uncertainties of the measured quantities in this research.

Parameter	Uncertainty	Units
Thermocouples	0.1%	*℃*
Power	1% of reading	kWm^{-2}
Refrigerant mass velocity	0.1% of reading	$kgm^{-2}s^{-1}$
Pressure sensors	1	*kPa*
Pressure drop transducer	0.075% of reading	*Pa*
Diameter	0.05	*mm*
Length	0.5	*mm*
Vapor quality	5%	-
Frictional pressure drop	4%	Pa

4. Results and discussion

In this part, firstly, the experimental pressure drop results of R-600a during forced convective evaporation in smooth and rough tubes are discussed. Then, the overall effectiveness of spiral

coils and the system performance are evaluated considering the current pressure drop results and the previous heat transfer results reported in [16]. Finally, a new correlation is suggested based on the current empirical results in order to predict the pressure drop of R-600a during evaporation within horizontal spring inserted pipes. Also, a sight glass was installed after the test section to observe the flow regimes. Generally, depending on the operational conditions of the system and tube sets, three flow patterns including stratified wavy, intermittent, and annular were observed. Fig. 2 demonstrates the observed flow regimes. However, at higher vapor qualities and mass velocities where the shear force between vapor phase and liquid phase dominates the body force, the annular flow pattern was dominant.

Stratified-wavy (G=109.2 kgm^{-2}s^{-1}, x=0.538)

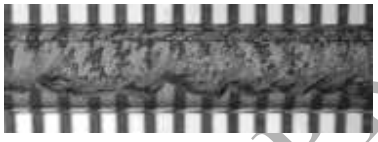

Intermittent (G=269 kgm^{-2}s^{-1}, x=0.349)

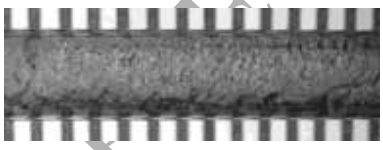

Annular (G=189 kgm^{-2}s^{-1}, x=0.778)

Fig. 2. The observed flow patterns in this study.

4.1.Pressure drop inside the plain and rough pipes

Fig. 3 demonstrates the trend of pressure drop growth with vapor quality in the plain pipe for various mass fluxes. The results show that increment of the vapor quality gives rise to the pressure losses. Indeed, as it was discussed by Aroonrat and Wongwises [25], by increasing the vapor quality, a larger velocity gradient is established between two phases of vapor and liquid. Therefore, the shear stress between two phases augments. Also, for any given vapor quality, obtained pressure losses are larger for higher mass fluxes. The reason is that the turbulence intensities of liquid and vapor phases would reach higher values when the mass flux grows, which in turn would result in further increase of the shear stress. As a result of above-mentioned factors, the pressure loss increases. Similar observations were reported in previous studies [26, 27]. Fig. 3 shows an uneven distribution of pressure drop data by increase of the mass flux. As it was discussed by Agrawal et al [28], forced convective two-phase flow is severely an unstable phenomenon since the vapor phase and liquid phase flow together which is accompanied by transformation of phases. What is more, installing spiral coils inside the pipe will also affect the

flow turbulence and the liquid film on the tube inner wall. These factors cause the unexpected distribution of pressure drop data.

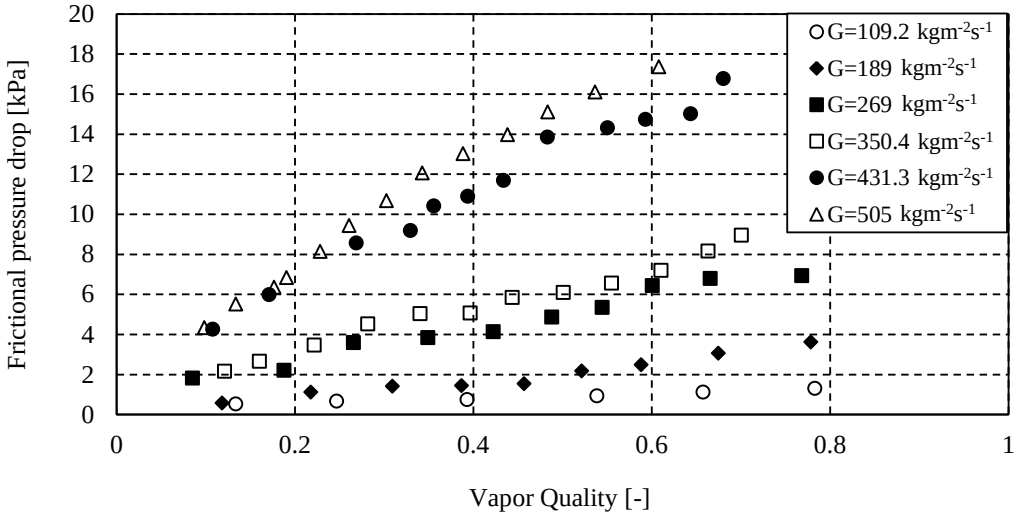

Fig. 3. The variations of frictional pressure drops with vapor quality in the plain tube for various mass fluxes.

In order to validate the present empirical results of the plain pipe, correlations suggested by Friedel [29], Chisholm [30], and Quiben and Thome [31] are considered. The comparison of the results obtained by experiments and the correlations is illustrated in Fig. 4. As can be seen, the relation proposed by Friedel [29] is more accurate than the other relation by predicting the most of the results within the error band of ±20%.

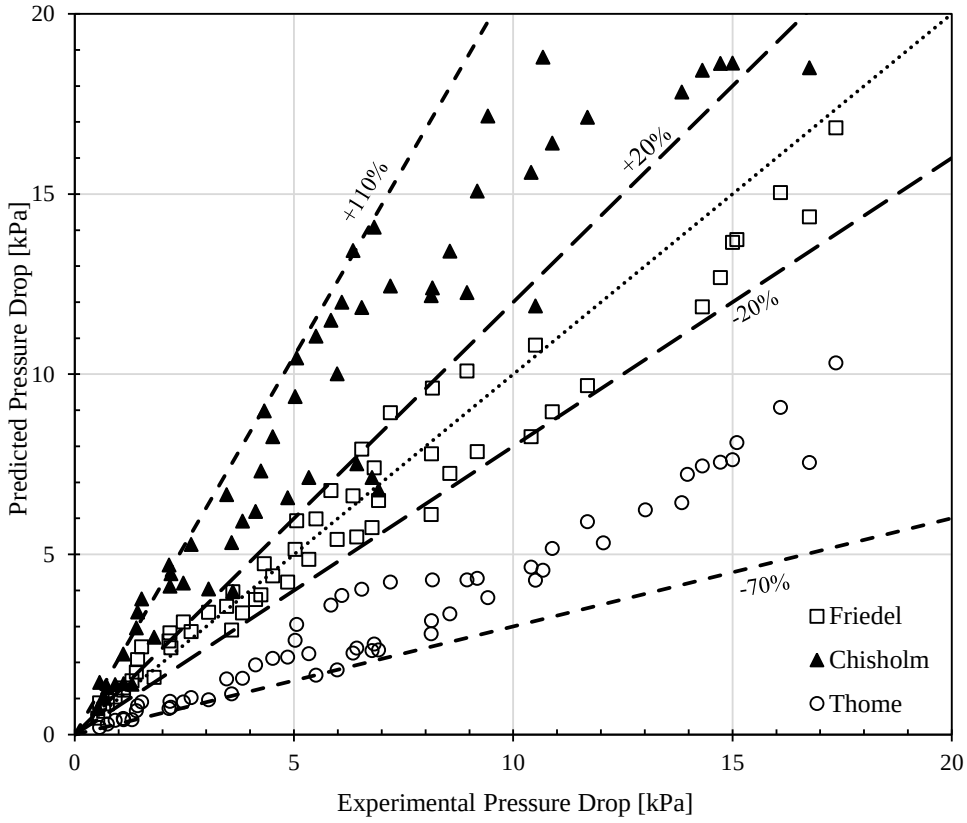

Fig. 4. The comparison of the obtained pressure drop values by the correlations and the experiments.

The variations of pressure drop for different mass fluxes as the vapor quality varies are shown in Figs. 5-9. It can be deduced from the plots that for all mass velocities, installing coiled wires induces higher pressure drop values compared to the smooth pipe. It is noticeable that the amount of pressure drop augmentation is related to the coiled wires type, vapor quality, and mass velocity.

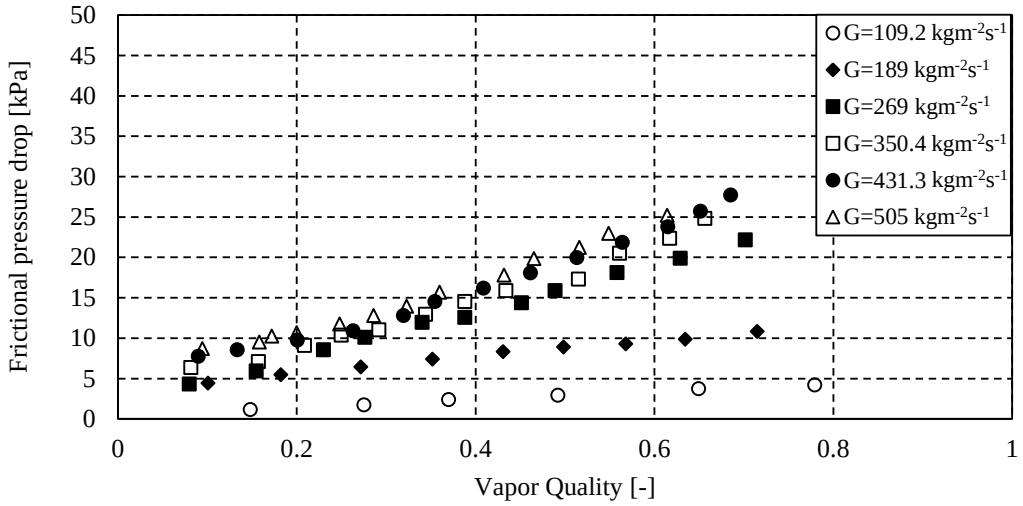

Fig. 5. The variations of frictional pressure drops with vapor quality for the tube set "CW1" under various mass fluxes.

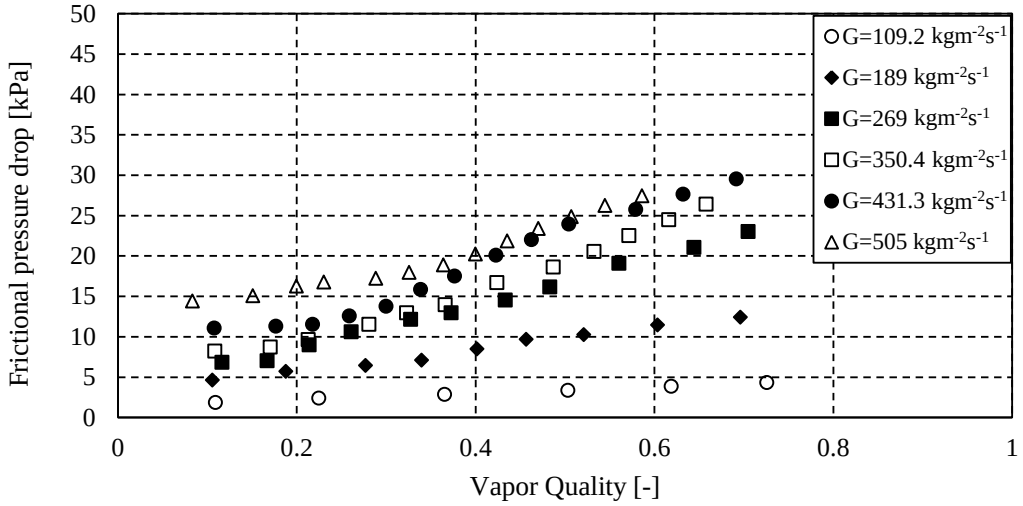

Fig. 6. The variations of frictional pressure drops with vapor quality for the tube set "CW2" under various mass fluxes.

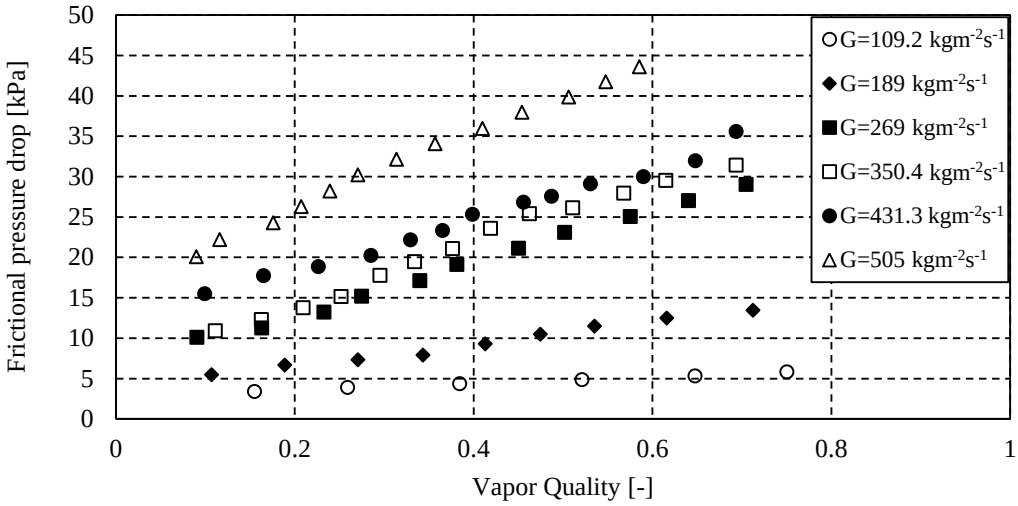

Fig. 7. The variations of frictional pressure drops with vapor quality for the tube set "CW3" under various mass fluxes.

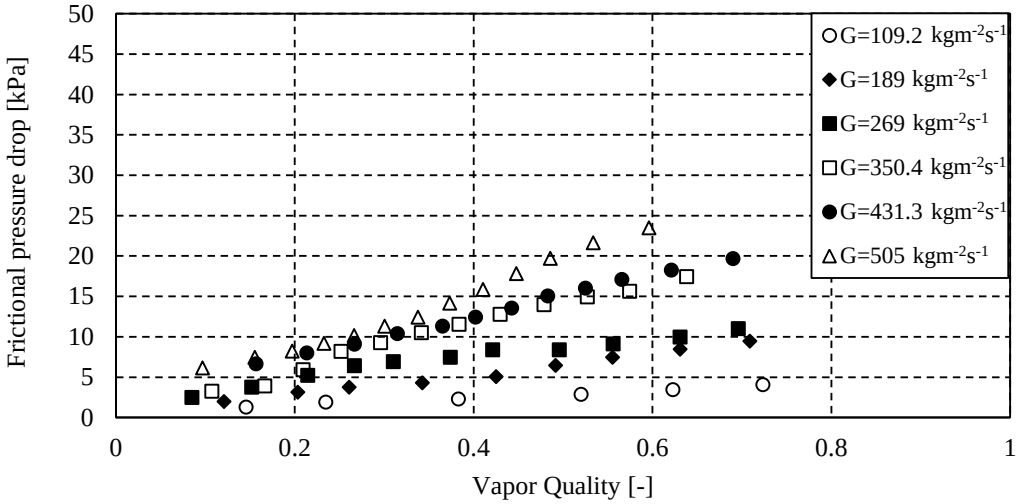

Fig. 8. The variations of frictional pressure drops with vapor quality for the tube set "CW4" under various mass fluxes.

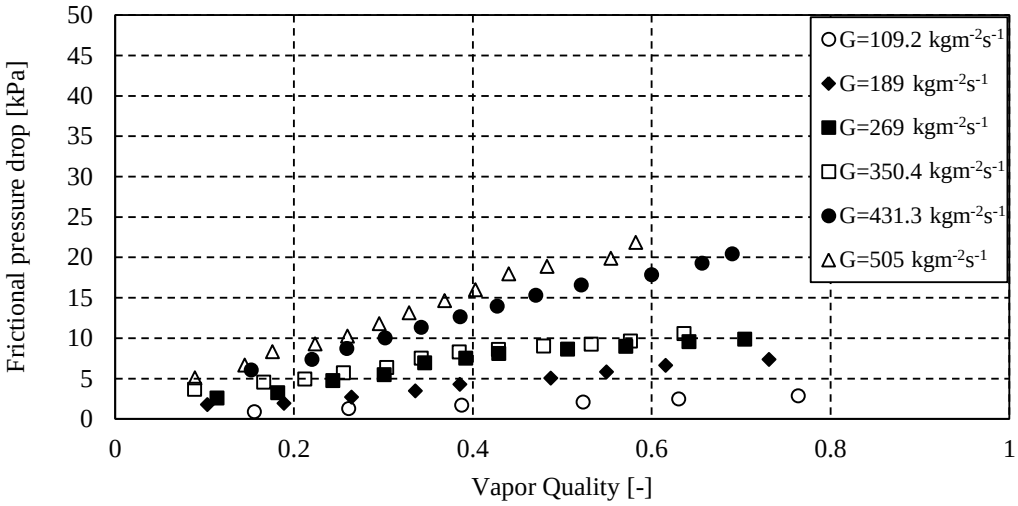

Fig. 9. The variations of frictional pressure drops with vapor quality for the tube set "CW5" under various mass fluxes.

According to Figs. 5-7 it can be found that as the wire become thicker, higher pressure losses are imposed to the system. These results are obtained for coiled wires with the identical coil pitch of 10 *mm* and various wire diameters of 0.5, 1, and 1.5 *mm*. Augmenting the wire diameter leads to increment of the frictional surface giving rise to the pressure drop. The other reason could be that the turbulence of liquid and vapor phases augments as the wire diameter increases. Furthermore, by installing thicker wire coils, the flow velocity augments due to the decrement of the flow cross-section area. It is also observable form these plots that the lowest and highest pressure drop rises of 90% and 958% over the plain pipe are obtained by using the tube set "CW5" at mass velocity of 109.2 $kgm^{-2}s^{-1}$ and tube set "CW3" at mass velocity of 505 $kgm^{-2}s^{-1}$, respectively.

Figs. 6,8,9 can be studied in order to compare the tubes pressure losses when spiral coils with identical wire diameter of 1 *mm* and varied coil pitches of 10, 20, and 30 *mm* are utilized. It is deducible from these figures that pressure drop rises by reducing the coil pitch because frictional surface per length of the test pipe augments.

According to the results, it can be seen that the trend of changes of the pressure drop data is not even for the inserts. In other words, the pressure drop results have been distributed unevenly. This is because the pressure drop results are a complex function of vapor quality, mass velocity, and geometry of tubes, and a general trend cannot be observed for all ranges of operating conditions and inserts.

To further illuminate the role of geometrical features of the coiled wires on the system pressure losses, Fig. 10 is drawn. In this regard, the parameter ($e/P^{1.5}d_e$) called coiled wire pressure drop index is defined which is directly proportional to the wire diameter and inversely related to the coil pitch (P) and equivalent diameter (d_e). The equivalent diameter is defined as:

$$d_e = {(d^2 - \gamma e)}\Big/{(d + \gamma)} \tag{12}$$

Where γ is computed as follows:

$$\gamma = {\pi e(d-e)}\Big/{(Psin\theta)} \tag{13}$$

Where θ represents coil helix angle.

A higher power is devoted to the coil pitch, because it was found by the experiments that changing the coil pitch has a prominent role in the pressure drop increase compared to changing the wire diameter. This figure demonstrates the pressure drop ratio of the rough pipes to the smooth pipe. It is found that the pressure drop amounts are strongly related to the inserts type. For any insert, the pressure drop reaches larger values as the coiled wire pressure drop index increases. As can be seen, the boundary of pressure drop increase is higher for the tube sets "CW1","CW2", and "CW3". This is because these coiled wires own the smallest coil pitch meaning higher index. However, among these three inserts, the tube set "CW3" imposes higher pressure drops as its wire diameter is larger.

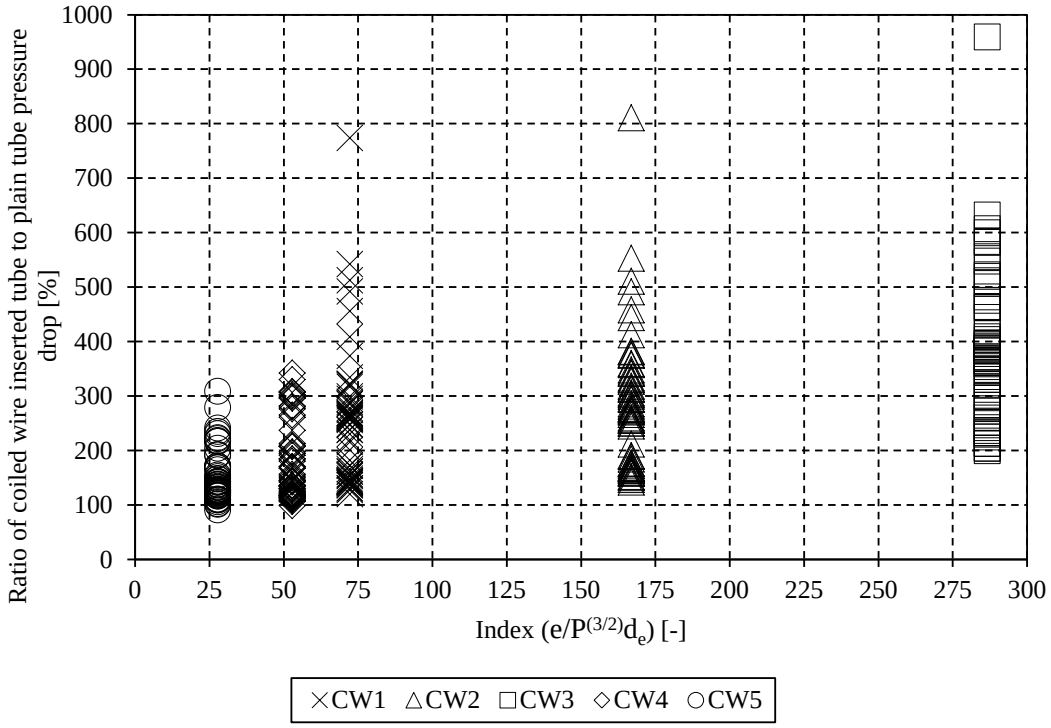

Fig. 10. The boundary of pressure drop increase with spiral coil index for all mass fluxes and vapor qualities.

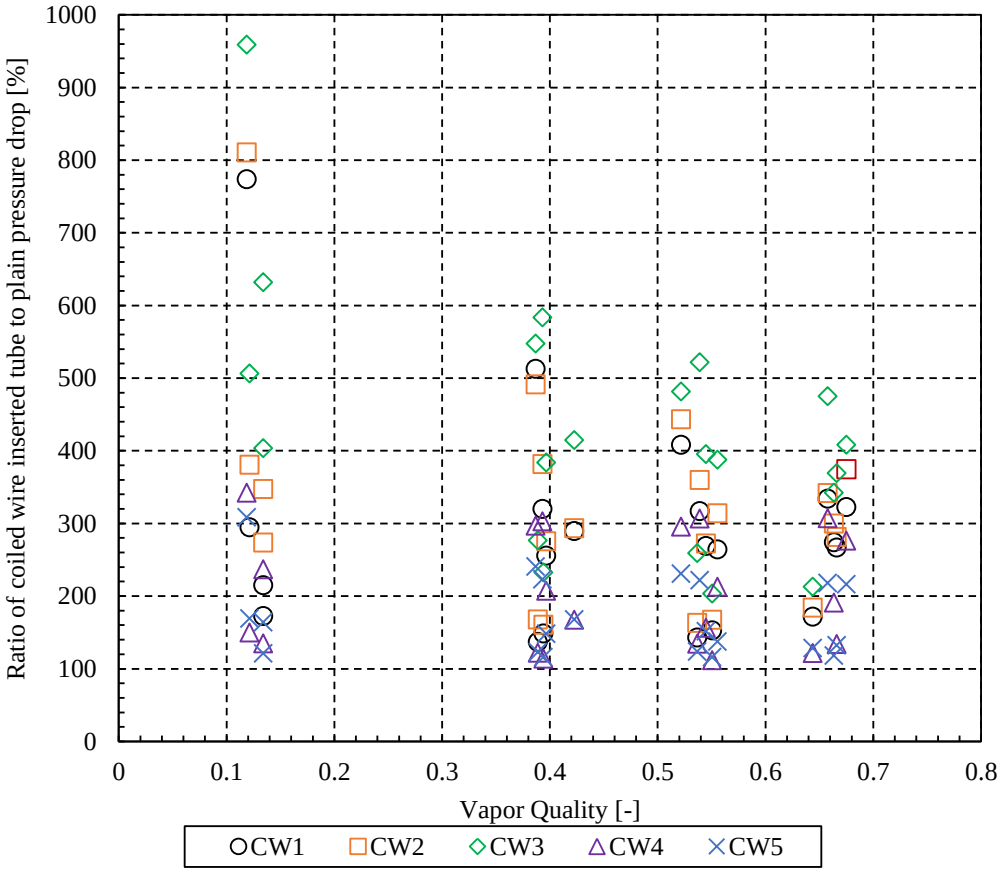

Fig. 11. The ratio of the rough pipes pressure drops to the smooth pipe pressure drops for various vapor qualities.

Fig. 11 shows the ratio of the obtained pressure drop by rough pipes to that of the smooth pipe for different vapor qualities. It can be seen from this plot that inserting coiled wires at lower vapor qualities results in higher pressure drops. As the vapor quality increases, the ratio of pressure drops decreases. It is deducible from this figure that using inserts at higher vapor qualities is more beneficial.

4.2.Performance assessment of rough pipes

The current empirical results showed that the inserts lead to the growth in pressure drop which is not preferable. On the other hand, as it was reported previously [16], these inserts contribute to the heat transfer coefficients enhancement which is favorable. The pressure loss and heat transfer coefficients are independent from each other and not related by an equation. Therefore, to evaluate the overall effectiveness of these instruments, a parameter called performance factor (PF) is introduced. In this regard, a new parameter defined by Agrawal and Varma [32] as the pumping power to the augmented heat transfer coefficient ratio is used in order to assess the system performance. The increase of pressure drop as a result of spiral coils gives rise to the pumping power. The pumping power can be calculated using the following relation:

$$W = \dot{v}\Delta P \tag{14}$$

Where, $\dot{v}$ and ΔP represent the volumetric flow rate and the pressure drop inside the test section, respectively.

In the current study, the ratio of consumed power by the pump to the smooth pipe heat transfer coefficient($^{W}/_{h})_s$, is computed. Then, the same ratio is determined for the spiral coil inserted or rough pipes($^{W}/_{h})_r$. Finally, the ratio of $(^{W}/_{h})_s$ to $(^{W}/_{h})_r$ as the performance factor is computed:

$$PF = \frac{(^{W}/_{h})_s}{(^{W}/_{h})_r} = \frac{^{h_r}/_{h_s}}{^{(\Delta P)_r}/_{(\Delta P)_s}} = {}^{R_h}/_{R_{\Delta P}} \tag{15}$$

In Eq. (15), R_h shows the heat transfer coefficient ratio of the rough pipe to the smooth pipe. Also, $R_{\Delta P}$ represents the pressure drop ratio of the rough pipe to the smooth pipe. To determine the effectiveness of springs, "PF" is used. If this parameter is larger than one, spiral coil usage is instrumental. Else, its usage is not helpful and recommended unless for specific conditions.

The performance factor is calculated and illustrated in Fig. 12 using inserts for all operating conditions. Fig. 12 shows that spiral coils usage significantly influences the system performance. Except "CW3", with the lowest pitch and highest wire thickness among all inserts, which induced the highest pressure drop, the other inserts improved the system performance. The best performance is presented by "CW5" having the wire diameter of 1 *mm* and coil pitch of 30 *mm*. By using this insert, the performance factor reached the highest value of 1.40. However, it is noticeable that the obtained values are also dependent of the mass velocity. To reveal the effects of both inserts and mass velocity simultaneously, Fig. 13 is presented. This plot demonstrates that inserts show the best performance at high mass fluxes. Using spiral coils is not beneficial at low mass velocities as the heat transfer enhancement is not large enough to negate the effects of pressure drop increment. Similar observations were reported by Akhavan-Behabadi et al. [33]. They studied the heat transfer and pressure loss of refrigerant R-134a during evaporation inside horizontal smooth and spiral coil inserted pipes for various vapor qualities and mass fluxes between 54-136 $kgm^{-2}s^{-1}$. For this range of the mass flux, it was observed that the system performance factor was below one. The results of current study also shows that using inserts at lower mass fluxes is not beneficial. On the contrary, at higher mass fluxes the heat transfer rate increases enough to overcome the adverse effects of pressure drop increase. It is also noticeable that at higher mass fluxes, the pressure drop ratio of the rough pipes to smooth pipes is smaller than that at lower mass fluxes. In other words, as it was explained by Nualboonrueng and Wongwises [34], the impacts of surface modifications in increasing the pressure drop at lower mass fluxes is much considerable. Considering Fig. 13, it is observed that generally coiled wires "CW4" and "CW5" having the larger pitches compared to the other inserts, perform better at higher mass velocities.

Different trends in variations of heat transfer and pressure drop with mass velocity have led to different performance factors. By taking into account the current pressure drop and previous heat

transfer data [16] and considering "CW5" as the best performing insert and for the vapor quality of about 0.5, by increasing the mass flux from 109.2 to 505 $kgm^{-2}s^{-1}$, the pressure drop ratio of the rough tubes to the smooth tube decreases from 2.17 to 1.24. This shows that the effects of inserts in augmenting the pressure drop at lower mas fluxes is much considerable. Also, for the same vapor quality and mass velocity range, the heat transfer coefficient ratio of rough pipes to plain pipe slightly increases from 1.4 to 1.45. Therefore, a higher performance factor is achieved at higher mass fluxes. So, it is recommended to use the inserts at higher mass fluxes.

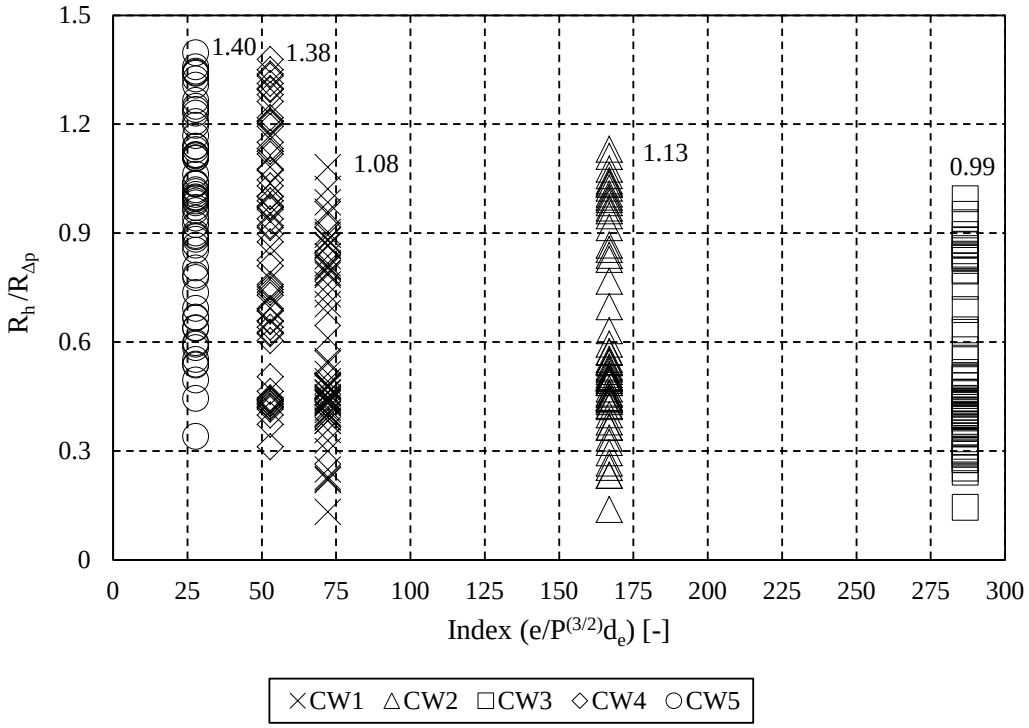

Fig. 12. The boundary of performance factor variations with spiral coil index for all mass fluxes and vapor qualities.

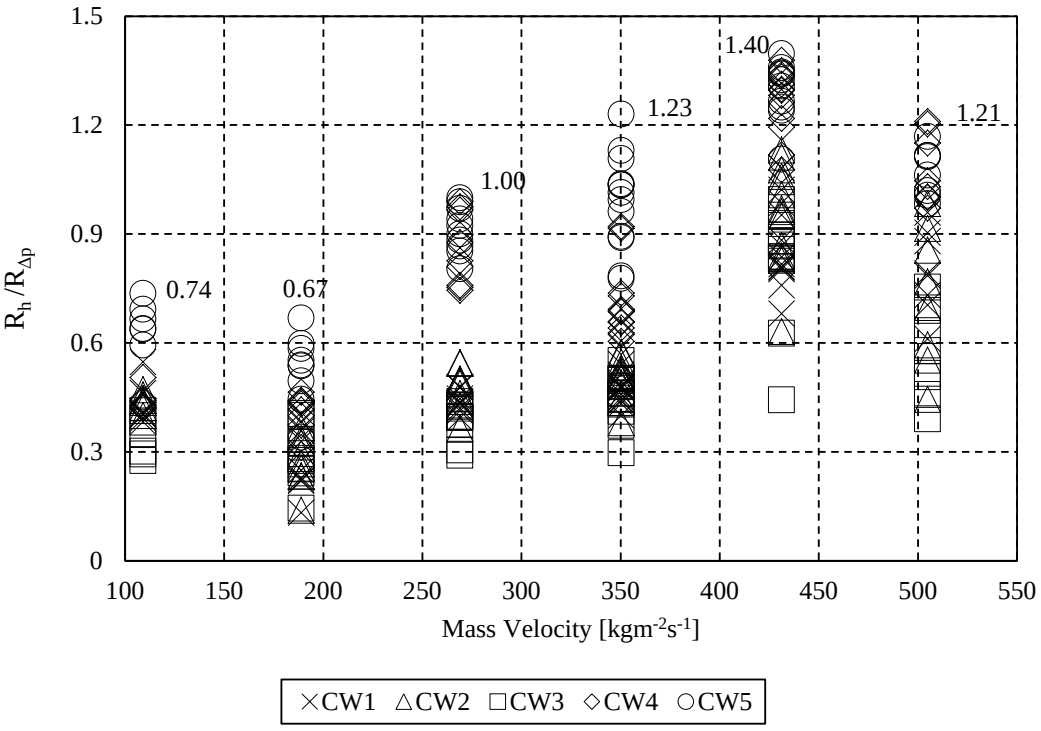

Fig. 13. The variations of performance factor with mass velocity for all inserts and various vapor qualities.

4.3. A new correlation for predicting the pressure drops in rough pipes

Different correlations have been developed previously in order to predict the pressure drop of heat-exchangers, since these relations can be useful in designing efficient heat-exchangers. As there is no correlation for predicting the forced convective evaporative pressure loss using R-600a within spiral coil inserted pipes, a new correlation is proposed based on the present experimental data.

To develop the new correlation, a proposed relation by Friedel [29] for predicting the pressure losses in plain tubes is utilized as the basic relation. Then, a dimensionless parameter, (e^2/Pd_e), is implemented for taking into account the impacts of geometrical parameters of spiral coils; and the following functional relationship is used:

$$\Delta P_r = \Delta P_s (c_1 + c_2 \frac{e^2}{Pd_e})^{c_3} \quad (16)$$

In Eq. (16), ΔP_r and ΔP_s represent the total pressure drop amounts in rough and smooth pipes, respectively. Also, d_e shows the equivalent diameter.

Regarding the nonlinear least square regression method, first, all the required data (320 data points) were transferred to the MATLAB Workspace according to parameters of the chosen fitting function, Eq. (16). Then, by means of Curve Fitting Toolbox, nonlinear regression, the fitting function of $z = y * (a + b * x)^c$ according to the aforementioned correlation was chosen

in which z stands for rough tube pressure drop, x is for the dimensionless parameter ($\frac{e^2}{Pd_e}$) and y is representing smooth tube pressure drop. Fitting optimization option was set to Bisquare for robustness with the aid of Levenberg-Marquardt Algorithm. After solving with 400 iterations for the set objective variables of $a = c_1$, $b = c_2$ and $c = c_3$ the convergence was reached for fitting optimization options. Finally, the Optimized coefficients (with 95% confidence bounds) were found. The new correlation is suggested as follows:

$$\Delta P_r = \Delta P_s(1.068 + 12.61\frac{e^2}{Pd_e})^{2.497} \quad (17)$$

The comparison between the results obtained by the current developed relation and the experimental results is demonstrated in Fig. 14. This plot shows that the new correlation is capable of predicting most of the pressure drop data in the error range of ±30%.

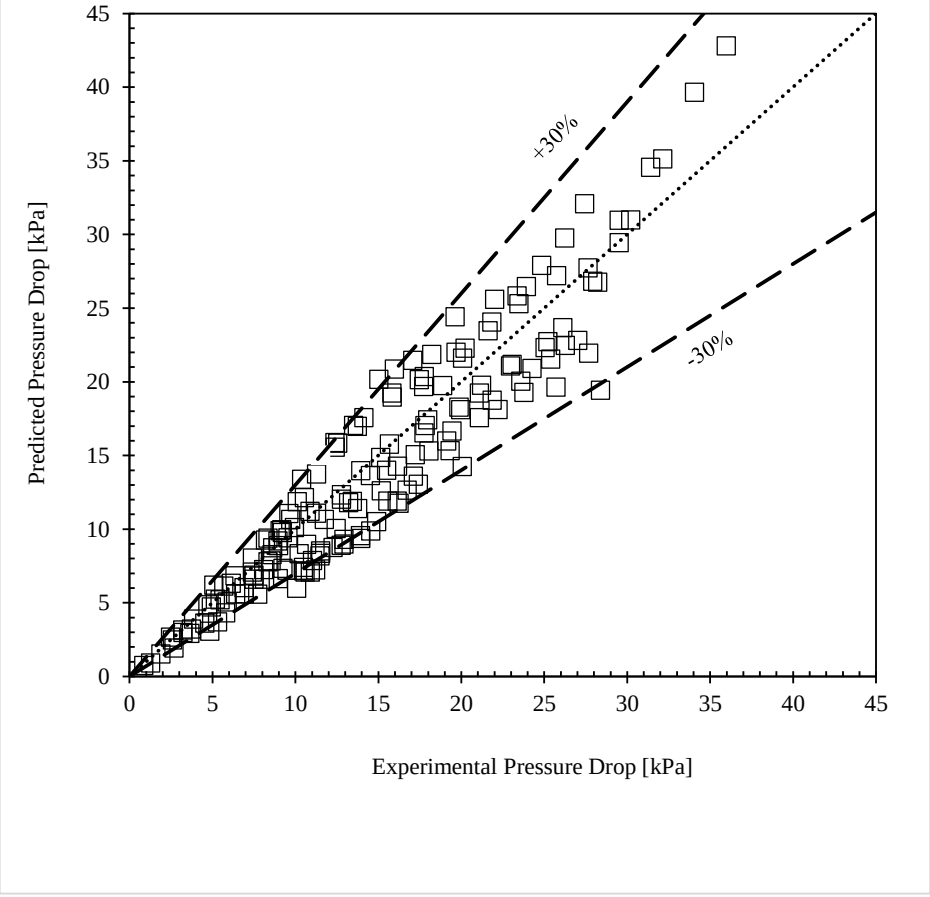

Fig. 14. The comparison of the pressure drops obtained by the new correlation and the experiments.

To calculate the average deviation (AD) and average absolute deviation (AAD) of the results obtained by the new correlation, Eq. (17), from the empirical results the following relations are used:

$$AD = \frac{1}{N}\left(\sum_{1}^{N}\frac{h_{calculated} - h_{experimental}}{h_{experimental}}\right) \times 100 \quad (18)$$

$$AAD = \frac{1}{N}\left(\sum_{1}^{N}\frac{\left|h_{calculated} - h_{experimental}\right|}{h_{experimental}}\right) \times 100 \quad (19)$$

Based on the calculations, it is observed that the average deviation and the average absolute deviation of the obtained results by the new correlation from the experimental results are -1.70% and 9.65 %, respectively.

5. Conclusion

An experimental setup is established to investigate the effectiveness of spiral coil inserts used inside horizontal pipes during forced convective evaporation of R-600a. For this purpose, circular cross-section spiral coils having varied wire diameters and coil pitches are employed. Also, different vapor qualities and mass fluxes are considered. The following conclusions are drawn from this research:

- Installing spiral coil inserts resulted in pressure loss augmentation for all vapor qualities and mass velocities.
- Increasing the mass velocity and vapor quality gave rise to the pressure drop.
- Pressure drop ratio of the rough tubes to smooth tubes is lower at higher mass fluxes.
- Employing coiled wires is beneficial at higher mass fluxes as the heat transfer enhancement could overweight the pressure drop growth.
- Using coiled wires at low vapor quality region results in higher pressure drops.
- The tube set “CW5” having the wire diameter of 1 *mm* and coil pitch of 30 *mm*, performed superior compared to the other inserts by maximum performance factor of 1.4.
- A new correlation was developed using the current experimental results to predict the pressure loss during evaporation of R-600a within horizontal spiral coiled inserted pipes.

6. Competing interests:

The authors have no competing interests to declare.

7. References:

[1] K. Aroonrat and S. Wongwises, "Experimental investigation of condensation heat transfer and pressure drop of R-134a flowing inside dimpled tubes with different dimpled depths," *International Journal of Heat and Mass Transfer,* vol. 128, pp. 783-793, 2019.

[2] S. Laohalertdecha and S. Wongwises, "Condensation heat transfer and flow characteristics of R-134a flowing through corrugated tubes," *International Journal of Heat and Mass Transfer,* vol. 54, pp. 2673-2682, 2011.

[3] T. Naulboonrueng, J. Kaewon, and S. Wongwises, "Two-phase condensation heat transfer coefficients of HFC–134a at high mass flux in smooth and micro-fin tubes," *International communications in heat and mass transfer,* vol. 30, pp. 577-590, 2003.

[4] H. A. Moghaddam, A. Sarmadian, and M. Shafaee, "An experimental study on condensation heat transfer characteristics of R-600a in tubes with coiled wire inserts," *Applied Thermal Engineering,* p. 113889, 2019.

[5] S. Ponnada, T. Subrahmanyam, and S. Naidu, "A comparative study on the thermal performance of water in a circular tube with twisted tapes, perforated twisted tapes and perforated twisted tapes with alternate axis," *International Journal of Thermal Sciences,* vol. 136, pp. 530-538, 2019.

[6] B. Kumar, G. P. Srivastava, M. Kumar, and A. K. Patil, "A review of heat transfer and fluid flow mechanism in heat exchanger tube with inserts," *Chemical Engineering and Processing-Process Intensification,* vol. 123, pp. 126-137, 2018.

[7] A. R. S. Suri, A. Kumar, and R. Maithani, "Convective heat transfer enhancement techniques of heat exchanger tubes: a review," *International Journal of Ambient Energy,* vol. 39, pp. 649-670, 2018.

[8] V. Özceyhan, "Conjugate heat transfer and thermal stress analysis of wire coil inserted tubes that are heated externally with uniform heat flux," *Energy conversion and management,* vol. 46, pp. 1543-1559, 2005.

[9] X. Zhuang, M. Gong, X. Zou, G. Chen, and J. Wu, "Experimental investigation on flow condensation heat transfer and pressure drop of R170 in a horizontal tube," *International Journal of Refrigeration,* vol. 66, pp. 105-120, 2016.

[10] Z.-Q. Yang, G.-F. Chen, Y.-X. Zhao, Q.-X. Tang, H.-W. Xue, Q.-L. Song*, et al.*, "Experimental study on flow boiling heat transfer of a new azeotropic mixture of R1234ze (E)/R600a in a horizontal tube," *International Journal of Refrigeration,* vol. 93, pp. 224-235, 2018.

[11] H. Moghaddam, M. Shafaee, and R. Riazi, "Numerical Investigation of a Refrigeration Ejector: Effects of Environment-Friendly Refrigerants and Geometry of the Ejector Mixing Chamber," *European Journal of Sustainable Development Research,* vol. 3, 2019.

[12] Z. Yang, M. Gong, G. Chen, X. Zou, and J. Shen, "Two-phase flow patterns, heat transfer and pressure drop characteristics of R600a during flow boiling inside a horizontal tube," *Applied Thermal Engineering,* vol. 120, pp. 654-671, 2017.

[13] K. A. Joudi, A. S. K. Mohammed, and M. K. Aljanabi, "Experimental and computer performance study of an automotive air conditioning system with alternative refrigerants," *Energy conversion and Management,* vol. 44, pp. 2959-2976, 2003.

[14] J. Copetti, M. Macagnan, and F. Zinani, "Experimental study on R-600a boiling in 2.6 mm tube," *international journal of refrigeration,* vol. 36, pp. 325-334, 2013.

[15] M.-Y. Wen, K.-J. Jang, and C.-Y. Ho, "The characteristics of boiling heat transfer and pressure drop of R-600a in a circular tube with porous inserts," *Applied thermal engineering,* vol. 64, pp. 348-357, 2014.

[16] M. Shafaee, F. Alimardani, and S. Mohseni, "An empirical study on evaporation heat transfer characteristics and flow pattern visualization in tubes with coiled wire inserts," *International Communications in Heat and Mass Transfer,* vol. 76, pp. 301-307, 2016.

[17] M. Shafaee, H. Mashouf, A. Sarmadian, and S. Mohseni, "Evaporation heat transfer and pressure drop characteristics of R-600a in horizontal smooth and helically dimpled tubes," *Applied Thermal Engineering,* vol. 107, pp. 28-36, 2016.

[18] A. Sarmadian, M. Shafaee, H. Mashouf, and S. Mohseni, "Condensation heat transfer and pressure drop characteristics of R-600a in horizontal smooth and helically dimpled tubes," *Experimental Thermal and Fluid Science,* vol. 86, pp. 54-62, 2017.

[19] J. D. de Oliveira, J. B. Copetti, and J. C. Passos, "Experimental investigation on flow boiling pressure drop of R-290 and R-600a in a horizontal small tube," *International Journal of Refrigeration,* vol. 84, pp. 165-180, 2017.

[20] Z.-Q. Yang, G.-F. Chen, Y. Yao, Q.-L. Song, J. Shen, and M.-Q. Gong, "Experimental study on flow boiling heat transfer and pressure drop in a horizontal tube for R1234ze (E) versus R600a," *International Journal of Refrigeration,* vol. 85, pp. 334-352, 2018.

[21] J. R. Thome, J. El Hajal, and A. Cavallini, "Condensation in horizontal tubes, part 2: new heat transfer model based on flow regimes," *International Journal of Heat and Mass Transfer,* vol. 46, pp. 3365-3387, 2003.

[22] J. G. Collier and J. R. Thome, *Convective boiling and condensation*: Clarendon Press, 1994.

[23] D. Steiner, "VDI-Wärmeatlas (VDI Heat Atlas)," *Verein Deutscher Ingenieure, VDI-Gesellschaft Verfahrenstechnik und Chemieingenieurwesen (GCV), Düsseldorf,* 1993.

[24] R. J. Moffat, "Describing the uncertainties in experimental results," *Experimental thermal and fluid science,* vol. 1, pp. 3-17, 1988.

[25] K. Aroonrat and S. Wongwises, "Condensation heat transfer and pressure drop characteristics of R-134a flowing through dimpled tubes with different helical and dimpled pitches," *International Journal of Heat and Mass Transfer,* vol. 121, pp. 620-631, 2018.

[26] K. Aroonrat and S. Wongwises, "Experimental study on two-phase condensation heat transfer and pressure drop of R-134a flowing in a dimpled tube," *International Journal of Heat and Mass Transfer,* vol. 106, pp. 437-448, 2017.

[27] S. Wongwises, S. Laohalertdecha, J. Kaew-On, W. Duangthongsuk, K. Aroonrat, and K. Sakamatapan, "Evaporation heat transfer and flow characteristics of R-134a flowing through internally grooved tubes," *Heat and Mass Transfer,* vol. 47, pp. 629-640, 2011.

[28] K. Agrawal, A. Kumar, M. A. Behabadi, and H. Varma, "Heat transfer augmentation by coiled wire inserts during forced convection condensation of R-22 inside horizontal tubes," *International journal of multiphase flow,* vol. 24, pp. 635-650, 1998.

[29] L. Friedel, "Improved friction pressure drop correlation for horizontal and vertical two-phase pipe flow," *Proc. of European Two-Phase Flow Group Meet., Ispra, Italy, 1979,* 1979.

[30] D. Chisholm, "Pressure gradients due to friction during the flow of evaporating two-phase mixtures in smooth tubes and channels," *International Journal of Heat and Mass Transfer,* vol. 16, pp. 347-358, 1973.

[31] J. M. Quibén and J. R. Thome, "Flow pattern based two-phase frictional pressure drop model for horizontal tubes, Part II: New phenomenological model," *International Journal of Heat and Fluid Flow,* vol. 28, pp. 1060-1072, 2007.

[32] K. Agrawal and H. Varma, "Experimental study of heat transfer augmentation versus pumping power in a horizontal R12 evaporator," *International journal of refrigeration,* vol. 14, pp. 273-281, 1991.

[33] M. Akhavan-Behabadi, S. Mohseni, H. Najafi, and H. Ramazanzadeh, "Heat transfer and pressure drop characteristics of forced convective evaporation in horizontal tubes with coiled wire inserts," *International Communications in Heat and Mass Transfer,* vol. 36, pp. 1089-1095, 2009.

[34] T. Nualboonrueng and S. Wongwises, "Two-phase flow pressure drop of HFC-134a during condensation in smooth and micro-fin tubes at high mass flux," *International communications in heat and mass transfer,* vol. 31, pp. 991-1004, 2004.